fermentation

MDPI

Article

Bioenergetic Modeling of the Relationship Between Voltage and Electroactive Microbial Biomass Yield for Bioelectrochemical Carbon Dioxide Reduction to Methane

Vafa Ahmadi and Nabin Aryal *

Department of Process, Energy and Maritime, University of Southeastern Norway, Kjølnes Ring 56, 3918 Porsgrunn, Norway; vafa.ahmadi@usn.no

* Correspondence: nabin.aryal@usn.no; Tel.: +47-3100-9386

Abstract: Optimal product synthesis in bioelectrochemical systems (BESs) requires a comprehensive understanding of the relationship between external voltage and microbial yield. While most studies assume constant growth yields or rely on empirical estimates, this study presents a novel thermodynamic model, linking anodic oxidation and cathodic carbon dioxide (CO_2) reduction to methane (CH_4) by growing microbial biofilm. Through integrating theoretical Gibbs free energy calculations, the model predicts electron and proton transfers for autotrophic methanogen and anode-respiring bacteria (ARB) growth, accounting for varying applied voltages and substrate concentrations. The findings identify an optimal applied cathodic potential of −0.3 V *vs.* the standard hydrogen electrode (SHE) for maximizing CH_4 production under standard conditions (pH 7, 25 °C, 1 atm) regardless of ohmic losses. The model bridges the stoichiometry of anodic and cathodic biofilms, addressing research gaps in simulating anodic and cathodic biofilm growth simultaneously. Additionally, sensitivity analyses reveal that lower substrate concentrations require more negative voltages than standard condition to stimulate microbial growth. The model was validated using experimental data, demonstrating reasonable predictions of biomass growth and CH_4 yield under different operating voltages in a multi substrate system. The results show that higher voltage inputs increase biomass yield while reducing CH_4 output due to non-optimal voltage. This validated model provides a tool for optimizing BES performance to enhance CH_4 recovery and biofilm stability. These insights contribute to finding optimum voltage for the highest CH_4 production for energy efficient CO_2 reduction for scaling up BES technology.

Keywords: thermodynamic model; microbial yield; acetate oxidation; methane production; electroactive biomass yield

Academic Editors: Thaddeus Ezeji and Miguel Ladero

Received: 12 December 2024
Revised: 6 January 2025
Accepted: 10 January 2025
Published: 17 January 2025

Citation: Ahmadi, V.; Aryal, N. Bioenergetic Modeling of the Relationship Between Voltage and Electroactive Microbial Biomass Yield for Bioelectrochemical Carbon Dioxide Reduction to Methane. *Fermentation* **2025**, *11*, 40. https://doi.org/10.3390/fermentation11010040

1. Introduction

The modeling and simulation of bioelectrochemical systems (BESs) have recently gained significant attention, integrating microbiology, electrochemistry, and reactor engineering. Several mathematical models have been developed to describe substrate degradation, microbial growth, and electron transfer mechanisms in BESs. The key parameters of BES models include substrate and biomass concentrations, biofilm thickness, current generation, and bioelectrochemical reaction kinetics, typically described using Nernst–Monod or Butler–Volmer equations [1]. These advancements have facilitated the optimization of BES configurations and operational strategies, such as reactor flow modes and electrode

arrangements, ultimately reducing construction and operation costs as well as extensive expenses related to testing various parameters separately [2].

Early models often assumed constant biomass density, whereas more recent studies incorporate variable biofilm growth, substrate diffusion, and dynamic electrochemical interactions. Effective mixing enhances substrate diffusion and improves nutrient distribution in the biofilm, consequently improving microbial metabolism and electron transfer. However, excessive mixing can generate shear stress on the electrode, leading to biofilm detachment, that could reduce bioelectrochemical performance [3,4]. Therefore, modeling efforts often include mixing intensity or biofilm detachment velocity as a key parameter to balance nutrient availability and biofilm integrity [5,6]. Electrode properties such as conductivity, surface area, and porosity also influence electron transfer efficiency and biofilm formation, which must be incorporated in BES modeling. Another critical aspect of BES modeling is the correlation between applied energy and product yield. In microbial electrochemical cells, the applied voltage directly impacts electron transfer driving forces, influencing both production efficiency and microbial growth rates [1,7]. While some studies have modeled microbial yield using coulombic efficiency and biofilm density [8], accurately quantifying microbial biomass yield in response to varying applied voltages remains a challenge. This highlights the need for more comprehensive models capable of predicting yield coefficients under diverse operating conditions [4].

BES modeling has progressed from simplified kinetic descriptions to integrate multiphysics frameworks, such as computational fluid dynamics and machine learning, to optimize system performance. However, gaps remain in accurately predicting microbial yield under different applied voltages, necessitating further research into parameter-specific models that account for reactor configurations, electrode materials, and biofilm behavior.

In the context of bioelectrochemical methane (CH_4) production, BES modeling offers significant benefits for process optimization. Different substrates lead to varying CH_4 yields in anaerobic digestion (AD) and BESs. Therefore, estimating biomass and product yield helps balance substrate input for enhanced CH_4 production [9]. The BESs address the deficiencies of conventional AD, such as low volumetric productivity, limited organic compound conversion, and inhibition due to the accumulation of volatile fatty acids (VFAs), ammonium, or sulfide [10–12]. BES can enhance CH_4 production through higher oxidation of organic compounds and improved CO_2 reduction to CH_4 [13]. However, these systems have not been fully scaled up due to energy efficiency concerns and unstable production [14].

The reduction of CO_2 to CH_4 in BES requires external overpotentials for bacteria and archaea to overcome potential losses. Organic matter typically serves as most frequent electron donor (substrate) for microorganisms. Nevertheless, reduced inorganic substances, such as ammonia, sulfide, and hydrogen (H_2), can also serve as electron donors, with CO_2 as the electron acceptor in energy metabolism. Oxidation-reduction reactions provide the energy that microorganisms need for growth and maintenance [15]. In these systems, electroactive methanogens take electrons from the solid electrode to reduce CO_2 to CH_4 [16].

In mediated electron transfer theories, the kinetics of electron transfer begins with anode-respiring bacteria (ARB), which oxidize organic compounds and provide electrons for the cathode. The biochemical mechanisms underlying extracellular electron transfer (EET) by ARB remain unclear. The most straightforward EET mechanism involves direct contact between the anode surface and the outer cell membrane cytochromes, where the general electron donor is used, and a solid acceptor substitutes the general electron acceptor, completing the catabolic reaction [17].

The growth kinetics of bioelectrochemical CO_2 reduction to CH_4 is essential for developing predictive models for AD and BESs [6,18]. One crucial aspect of microbial growth

processes is the Gibbs energy dissipation required to produce 1 mol of biomass when utilizing CO_2 as a carbon source. Calculating the bioenergetics of methanogenic reactions helps identify optimal operating conditions. Two approaches are conventionally used to establish the stoichiometry of biological CH_4 production: the empirical approach, based on molar empirical biomass yield, and the theoretical approach, corresponding to thermodynamic biomass formation and electron equivalent reactions. The empirical approach is simpler to apply when calculating biomass growth stoichiometry, whereas the theoretical approach is more detailed and relates Gibbs free energy to the biomass growth stoichiometry based on electron equivalent reactions [19,20]. However, there is a lack of clarity regarding which method is more straightforward and how it should be implemented in bioelectrochemical growth modeling to relate biomass yield to applied voltage. Understanding these relationships is essential for developing growth yield models for both anodic and cathodic biofilms. This is a primary step for implementing such models in various software to predict CH_4 production under different operating conditions. External energy inputs at optimum levels increase the microbial community of anodic oxidizing bacteria and enhance methanogenic biomass activity. Estimating the theoretical optimum voltage in BESs helps identify ohmic losses in the reactor, which are influenced by factors such as electrode material, configuration, and electrolyte characteristics. Consequently, regulating the concentration of organic and inorganic compounds can help reduce potential losses [5].

In most dynamic simulations, only bioanodes or biocathodes are simulated. To the knowledge of authors, no model attempted to connect bioanodic oxidation to the biocathodic reduction. The biomass yield on the biofilm in the BES system is taken from other literature, and the voltage at which the biofilm growth is maximum, is taken as an assumption in most papers [6,21–24]. To make the validation applicable, a method based on thermodynamics should be presented to calculate the electroactive biomass yield.

This study presents a novel investigation into the thermodynamic evaluation of how external voltage impacts biomass yield and CH_4 production in electro-reductive systems involving ARB and methanogens. Additionally, it establishes stoichiometric frameworks for CH_4 production by autotrophic methanogens and bioelectrochemical processes, emphasizing the application of Gibbs free energy for reaction modeling. To obtain this objective, the stoichiometry of autotrophic CH_4 production should be understood. Then, the stoichiometric growth of electroactive biofilm must be developed using the proper method to obtain the biomass yield on the biofilm at different voltages with respect to bioenergetics. This research advances the understanding of BES dynamics and offers a more precise approach to designing efficient CH_4 production in BES.

2. Theory, Methods, and Assumptions

Empirical and theoretical approaches were applied to obtain the stoichiometry of autotrophic microbial growth reaction for H_2 as electron donor and CO_2 as the inorganic carbon source as electron acceptor. Then, the stoichiometric growth reactions for 1 mol biomass via the two approaches were compared and the method that could be applicable in bioelectrochemistry was selected. The selected approach was used to establish the stoichiometry of growth for anodic biofilm growth and the stoichiometric metabolism of cathodic biofilm, where CH_4 is produced. The thermodynamic model was established in the Microsoft Excel solver spreadsheet-based program to relate the stoichiometry of biofilm growth to the voltage applied on the cathode and electroactive methanogen growth reaction. In addition, the effect of non-STD conditions on the applied voltage, biomass yield and CH_4 production was assessed. Then, the model was validated with experimental data from a BES reactor.

2.1. Empirical Method (Approach-1)

The biomass formula for the biomass growth is defined as $CH_{1.8}O_{0.5}N_{0.2}$. In approach-1, the autotrophic anabolic reaction based on inorganic carbon consumption (Equation (1)) is:

$$f \cdot CO_2 + a \cdot mol\ electron\ donor + b \cdot N - source + 1 \cdot CH_{1.8}O_{0.5}N_{0.2} + d \cdot H_2O + e \cdot oxidized\ electron\ donor + c \cdot H^+ \quad (1)$$

In this method, the conservation of elements and charge (electrons) should be fulfilled for the stoichiometric reaction. Thus, the stoichiometry of anabolism and the molar aquired biomass differs by varrying the carbon and electron source [19]. The anabolic reaction needs energy from the catabolic redox reaction. An electron acceptor and an electron donor engage in a redox reaction during catabolism which is connected to the conservation of energy in form of adenosine triphosphate (ATP) [17]. Biochemically, ATP is the main Gibbs energy carrier which delivers energy for anabolism and cell growth. The catabolic reaction is defined per mole electron donor oxidized. The overall growth reaction is given in Equations (2) and (3):

$$Overall\ growth\ reaction = Anabolism + f_{cat} \cdot Catabolism \quad (2)$$

$$f_{cat} = -Y_D^{Ogr} + Y_D^{an} = \underbrace{\frac{mol\ substrate\ consumed}{mol\ biomass\ produced}}_{\frac{1}{biomass\ yield}} + Y_D^{an} \quad (3)$$

where, Y_D^{an} is the stoichiometric coefficient of the electron donor in the anabolic reaction. $-Y_D^{Ogr}$ is obtained from $\frac{1}{biomass\ yield}$ assuming 1 mol/L acetate in the system at STD condition [19]. The yield of autotrophic methanogens was assumed as 0.05 and 0.2 g *biomass/g carbon source* as a low and high biomass yield for comparison [15,25].

2.2. Theoretical Method (Approach-2)

In approach-2, when microorganisms use CO_2 as a carbon source, a fraction of electrons as a source of energy (f_e^0) *is* transferred to the electron acceptor to provide energy for conversion of the other fraction of electrons (f_s^0) into microbial cells. The electrons in f_s^0 are transferred to the acceptor to produce more energy, and another portion is transformed into an inactive organic cell residue as cells degrade due to normal maintenance or predation. The general equation to obtain the cell structure is given in Equation (4):

$$\frac{(n-c)}{d} CO_2 + \frac{c}{d}\ HCO_3^- + \frac{c}{d}\ NH_4^+ + H^+ + e^- + \frac{1}{d} CH_{1.8}O_{0.5}N_{0.2} + \frac{(2n-b+c)}{d}\ H_2O \quad (4)$$

where $d = 4n + a - 2b - 3c$.

In this approach, all calculations are according to mol electron equivalent per mol product. Equations (5) and (6) give the overall biological reaction in approach-2:

$$R = f_e R_a + f_s R_{CS} - R_d \quad (5)$$

$$f_e + f_s = 1 \quad (6)$$

where,

- f_e is the fraction e^- mol of substrate oxidized per e^- mol of substrate used for catabolism.
- R_a is electron acceptor half-reaction (based on one mol electron equivalent).
- f_s is the fraction e^- mol of substrate used for cell synthesis (anabolism).
- R_{CS} is cell synthesis half-reaction (based on one mol electron equivalent).
- R_d is electron donor half-reaction (based on one mol electron equivalent).

Two phases are involved in the microbial yield from substrate use. The energy process first produces high-energy carriers like ATP. The energy carriers are secondarily spent to promote cell synthesis or cell maintenance. Every transfer result in a small loss of Gibbs free energy. The losses are not included in calculating the energy dissipation of cell formation to obtain the theoretical yield. Along with how to account for energy loss during transfers, the true yield (f_s^{real}) can be obtained from experimental data in various condition. Calculation of f_s^0 for the genuine biomass yield is possible applying thermodynamics and Gibbs free energy of half-reactions involved in the microbial growth reaction. So, the energy for maintenance is set to zero to ensure that all energy is used for cell synthesis. When the nitrogen source is ammonium, the energy needed to create one equivalent of cells from a given carbon source is ΔG_s. The energy shift caused by the transformation of the carbon source into the typical organic intermediates (for example, Pyruvate). The half-reaction of pyruvate formation (Equation (7)) is:

$$\frac{1}{5}CO_2 + \frac{1}{10}HCO_3^- + H^+ + e^- \rightarrow \frac{1}{10}CH_3COCOO^- + \frac{2}{5}H_2O \qquad \Delta G^0 = 35.09\ \text{kJ/e}^-\ \text{eq} \tag{7}$$

ΔG_p in Equation (8) is the energy of converting the carbon source to pyruvate:

$$\Delta G_P = 35.09 - \Delta G_c^{0'} \tag{8}$$

For autotrophs, inorganic carbon must be reduced to pyruvate using a lot of energy. Following that, pyruvate carbon is changed into cellular carbon. During electron transfer, energy is always lost. By inserting a term for energy-transfer efficiency ε, the loss is considered. In conclusion, the amount of energy needed for cell production is obtained by Equations (9)–(12):

$$\Delta G_s = \frac{\Delta G_p}{\varepsilon^n} + \frac{\Delta G_{pc}}{\varepsilon} \tag{9}$$

$$A = \frac{f_e^0}{f_s^0} = \frac{-\Delta G_s}{\varepsilon\left(\Delta G_r^0\right)} \tag{10}$$

and

$$f_e^0 = 1 - f_s^0 = \frac{A}{1+A} \tag{11}$$

$$f_s^0 = \frac{1}{1+A} \tag{12}$$

where,

- ΔG_s is energy for cell synthesis from a specific carbon source (kJ/e$^-$ eq).
- ΔG_p is energy required to convert carbon source to pyruvate (kJ/e$^-$ eq).
- ΔG_{pc} is energy required to convert pyruvate carbon to cellular carbon (kJ/e$^-$ eq).
- ε is energy capture efficiency, typically 55 to 70% under optimum conditions (ε = 0.6)
- n is energy transfer efficiency to convert carbon to pyruvate. n = +1 if $\Delta G_p > 0$ (energy is consumed), and $n = -1$ if $\Delta G_p < 0$ (energy is produced)
- ΔG_r^0 is the Gibbs free energy of exergonic reaction (kJ/e$^-$ eq).
- A is the equivalent electron donor which must be oxidized (energy of maintenance is not considered).

The energy transfer efficiency can vary at different conditions with diverse microbial types. Some microorganisms lack highly efficient enzyme systems which imply $\varepsilon < 0.6$. In general, microorganisms with a low ε are not anticipated to survive well in mixed cultures. In approach-2, the theoretical biomass yield will be estimated according to thermodynamics in STD conditions. It can differ from the real yield obtained from experiments at non-STD operating conditions. The concentrations of components, the microbial species, mixing, flow rate, pressure and temperature are some important parameters affecting the biomass yield [17].

The required reactions for CH_4 production are given in Equations (13)–(15) at standard conditions (pH 7, atmospheric pressure, 25 °C and 1 mol/L of components) [16].

$$\tfrac{1}{8}CO_2 + H^+ + e^- \rightarrow \tfrac{1}{8}CH_4 + \tfrac{1}{4}H_2O \qquad E^0 = -0.24\ \text{V vs. SHE}, \quad \Delta G^0 = +23.53\ \text{kJ/e}^-\ \text{eq} \tag{13}$$

$$H^+ + e^- \rightarrow \tfrac{1}{2}H_2 \qquad E^0 = -0.42\ \text{V vs. SHE}, \quad \Delta G^0 = +39.87\ \text{kJ/e}^-\ \text{eq} \tag{14}$$

$$\tfrac{1}{8}CO_2 + \tfrac{1}{2}H_2 \rightarrow \tfrac{1}{8}CH_4 + \tfrac{1}{4}H_2O \qquad \Delta E_{cell}^0 = +0.169\ \text{V}, \quad \Delta G_r^0 = -16.34\ \text{kJ/e}^-\ \text{eq} \tag{15}$$

By far, the most popular and beneficial electron donor is acetate. The half-reaction of acetate oxidation is given by Equation (16) [26]:

$$\frac{1}{8}CH_3COO^- + \frac{3}{8}H_2O \rightarrow \frac{1}{8}CO_2 + \frac{1}{8}HCO_3^- + H^+ + e^- \qquad \begin{matrix}\Delta G^0 = -27.68\ \text{kJ/e}^-\ \text{eq} \\ E^0_{ox} = +0.2839\ \text{V SHE}\end{matrix} \tag{16}$$

2.3. Gibbs Free Energy of Catabolism and Anabolism Reactions

It is crucial to estimate the Gibbs energy of catabolism because it provides Gibbs energy for metabolic growth. The Gibbs free energy for the growth reaction at standard condition can be calculated by Equation (17). The G_f^0 values in STD conditions (1 mol/L component, 25 °C, and 1 atm) can be found in Supplementary Materials (Table S3) [19,27].

$$\Delta G^0 = \sum G^0_{f,i,\ products} - \sum G^0_{f,i,\ reactants} \tag{17}$$

The catabolic reaction is affected directly by changes in concentration and temperature. The released ΔG will affect microbial growth and biomass yield. Assume a general catabolic reaction as $a\text{A} + b\text{B} \rightarrow c\text{C} + d\text{D}$ with standard Gibbs free energy as ΔG^0_r. Change in ΔG^0_r can be calculated by Equation (18).

$$\Delta G_r = \Delta G^0_r + RTln\frac{[\text{C}]^c[\text{D}]^d}{[\text{A}]^a[\text{B}]^b} \tag{18}$$

where R is the ideal gas constant 8.314 (J/k/mol), T is temperature (K), and the values in brackets correspond to concentration (mol/L).

The interface of electrochemistry and microbial biochemistry requires an awareness of the relationship between the potential difference (ΔE, V) and the free energy (ΔG, kJ/mol) as shown in the Nernst equation (Equation (19)):

$$\Delta G = -nF\Delta E \tag{19}$$

where ΔG is the Gibbs free energy (kJ/e$^-$ eq), n is the number of electrons, F is the Faraday constant 96.485 (kJ/V/e$^-$ eq), and ΔE is the potential difference in the cell [28].

2.4. Implementing Bioenergetics on Electroactive Biofilm Growth

A primary step for simulation of biofilm models is to assess bioenergetics of bioelectrochemical CH_4 production corresponding to the applied voltage through relating the anodic biofilm to the stoichiometric growth of cathodic biofilm. The activity of electroactive cathodic biofilm is limited by the number of electrons and H^+ flowing from anode to cathode. The assumptions for calculating the stoichiometry of electroactive biofilm growth are as follows:

- Atmospheric pressure is assumed for the entire model.
- The anodic and cathodic media are well mixed.
- Only bioelectrochemical oxidation and reduction are emphasized.
- Negative applied voltage on cathodes is assumed.
- A well-grown ARB biofilm which can oxidize acetate as substrate (electron donor) and deliver electrons to anode (electron acceptor) is assumed.
- The well-developed methanogenic biofilm on cathode takes electrons from cathode (electron donor) and reduces CO_2 and H^+ to CH_4.
- No electrons are lost in other reactions, and potential losses in the system due to ohmic resistances and reactor design are ignored.
- Electrode material and the self-potential of the electrode are not considered.
- HCO_3^-, and CO_2 are considered in equilibrium

Figure 1 illustrates the assumption for establishing the stoichiometric metabolic model of electroactive microbes in a double chamber or single chamber reactor. It illustrates that two complete metabolic reactions take place; one on anode and the other on cathode.

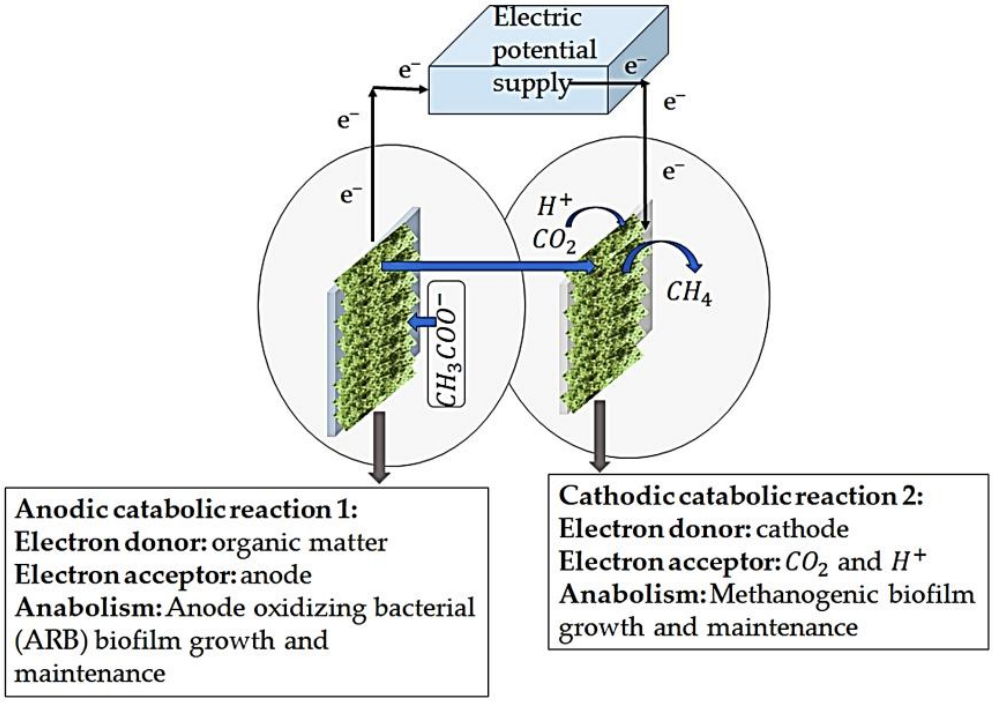

Figure 1. Graphical view of catabolism and anabolism in a bioelectrochemical reactor.

The thermodynamic model in this work was established for cathodic voltage of −0.25 V to −0.8 V *vs*. SHE. When ohmic resistances are ignored, the negative applied voltage on cathode can be interpreted as positive applied voltage on anode [29]. $f_e^0 = 1 - f_s^0 = \frac{A}{1+A}$ changes by change in voltage. The equivalent electron donor value (A) is relevant to f_e^0 and f_s^0. In STD condition, ΔG_r^0 of the catabolism (Equation (20)) is [27]:

$$\Delta G_r^0 = \Delta G_{oxidation}^0 + \Delta G_{reduction}^0 \quad (20)$$

$\Delta G_{oxidation}^0$ is normally given in reduction half reaction in thermodynamic reference books. Thus, the oxidation reaction and ΔG values of half reaction should be reversed. Therefore, for ΔG_r^0, $\Delta G_{oxidation}^0$ is acetate oxidation, but anode, which is a solid electron acceptor, do not have a typical $\Delta G_{reduction}^0$. Instead, the anode has an electric potential. Regardless of the self-potential of anode, anodic potential can be controlled by an external voltage to transfer electrons and the oxidized components for CH_4 production. In BESs, the anode and cathode are connected and CH_4 production has an optimum voltage. If a negative voltage is applied on cathode, $\Delta G_{reduction}^0$ is positive according to Nernst equation. So, negative voltage should be applied on cathode to make the reduction reaction spontaneous. According to this, Equations (21) and (22) define the potential difference:

$$\Delta E_{r,\,anode} = E_{final} - E_{initial} \quad (21)$$

which means:

$$\Delta E_{r,anode} = E_{anode} - E_{acetate\ oxidation} \quad (22)$$

The applied voltage on the electrode is relevant to ΔG by Nernst equation (Equation (19)). $E_{initial}$ is the voltage of acetate oxidation half reaction (+0.2839 V in STD conditions), while E_{anode} is the reverse value of the applied cathodic voltage regardless of losses [28,29]. On cathode, the electron donor is a solid cathode, and the electron acceptors are CO_2 and H^+. In this case, $\Delta G_p = 35.09 - \Delta G_{cathode}$. On cathode, ΔG_p, ΔG_s, and ΔG_r^0 vary by changing the applied potential. $\Delta G_{cathode}$ is obtained from Nernst equation according to the applied voltage on cathode, which is given in Equation (23).

$$\Delta E^0_{r,\,cathode,\,electron\ donor} = E^0_{CO_2\ reduction} - E^0_{cathode} \quad (23)$$

Deviating the concentrations from STD conditions changes the BES cell potential. Assume the reaction $aA + bB \rightarrow cC + dD$. To calculate the concentration over-potential, the entire reaction can be expressed using Equation (24) [28]:

$$\Delta E_{conc} = -\frac{RT}{8F} ln \frac{[A]^a_{anode}[B]^b_{anode}}{[C]^c_{cathode}[D]^d_{cathode}} \quad (24)$$

In biological environments, high acetate concentrations lead to oversaturation of the acetate oxidizing bacteria, that in turn, results in inhibition of the oxidation process. On the other hand, high amounts of CO_2 and H^+ may lead to a pH imbalance and oversaturation of the methanogenic biofilm on cathode [15,30]. Thus, acetate (CH_3COO^-) concentration was calculated for 0.5, 1.5, and 2.5 g/L. Also, the effect of temperature variations on the biomass yield and cathode potential for 25, 35, 45, and 55 °C at constant concentration was calculated for the anodic and cathodic biofilm.

2.5. Validation and Implementing the Model in a Complex BES System

To implement and validate the model with a more complex system, the model was used to estimate the yield of ARB and methanogens in a laboratory scale reactor of another work with heat-treated stainless-steel grade 314 as the anode and grade 316 as cathode material. The microbial media consisted of a complex media including acetic acid (CH_3COOH), soluble CO_2 (added as $NaHCO_3$), and soluble chemical oxygen demand (SCOD). The single chamber BES reactor had a well-developed anodic and cathodic biofilm. Additionally, the bioanode and biocathode potential in open circuit voltage (OCV) condition was reported to be average -0.43 V *vs*. SHE for biocathode and -0.4 V *vs*. SHE for bioanode. The data used in this paper were taken from that experimental study from the final week of CCV1 (applied -0.6 V *vs*. SHE) and CCV3 (applied -0.7 V *vs*. SHE) operations. The average daily results from the experimental study are given in Table 1 [31].

Table 1. The extracted data from an experimental study to calculate the bioenergetics of bioanode and biocathode in a single chamber BES reactor.

Parameters	**Value**	
Applied voltage on cathode (V *vs*. SHE)	−0.6	−0.7
Anodic potential response (V *vs*. SHE)	−0.34	−0.24
Relative anodic voltage considering to OCP (V *vs*. SHE)	+0.06	+0.16
Average daily CH_4 production (ml/L/d)	215	130
Average SCOD consumption (mg/L/d)	264	136
Average acetic acid consumption (mg/L/d)	80	No acetic acid content
Average CO_2 consumption (g/L)	0.41	0.41

Acetic acid value is equal to 1.32 mmol/L/d, the molar CO_2 value is 4.8 mmol/L/d, and the molar CH_4 values are, respectively, 8.8 mmol/L/d and 5.3 mmol/L/d. The molar value of protein assumed as the SCOD is 0.8 mmol/L/d and 0.386 mmol/L/d.

The data in Table 1 was used to establish the yield of methanogens and ARB. In a complex microbial media, especially in single chamber designs, calculating the yield of biofilm requires opening the reactor and take samples directly from the electrode, which may disturb the biofilms due to air exposure. This model helps to estimate the daily biofilm yield in different steps of the operation. In this work, the yield was calculated for 1 week in order to compare the effect of the applied voltage on biomass and CH_4 yield.

SCOD can be the source of CO_2 and H^+ in the system. The analysis in the experimental study shows that protein compounds (including amino acids, proteins, and nitrogenous organics) can be a strong candidate as the SCOD, corresponding to degradation reaction shown in Equation (25) [15]:

$$\frac{8}{33}CO_2 + \frac{2}{33}NH_4^+ + \frac{31}{33}H^+ + e^- \rightarrow \frac{1}{66}C_{16}H_{24}O_5N_4 + \frac{27}{66}H_2O \qquad \begin{matrix} \Delta G^0_{ox} = 32.22 \text{ kJ/e}^- \text{ eq} \\ E^0_{ox} = +0.33 \text{ V } vs. \text{ SHE} \end{matrix} \quad (25)$$

As reported in the experimental study, SCOD oxidizers were enriched on anode as one type of ARB. The acetate consuming bacteria were also found on anode. Nonetheless, as stated in the experimental study, a part of CH_4 production has taken place in the suspended media by taking electrons directly from anode, in addition to the cathodic methanogens. For simplicity, in this study, it

is assumed that the entire CH_4 production occurs on cathode. Moreover, in this real complex system, the source of H^+ was not only from SCOD and acetate oxidation. According to the mass balance, water reduction mechanisms were most probably active in the system to provide extra H^+ for CO_2 reduction to CH_4.

It should be noted that in a real BES reactor, extra potential due to ohmic resistances and the intrinsic potential of the electrode material leads to applying higher voltage on the working electrode. Measurements of anode and cathode potential in stable mode is important to calculate the relative positive potential of anode for microbial growth. For cathodic microbial growth, the exact applied voltage on cathode should be considered to include the losses in the model.

3. Results and Discussions

3.1. Stoichiometry of Biological CO_2 to CH_4 Conversion by Approach-1

The electron donor can be from different sources for autotrophic methanogens growing on CO_2, and H_2 can be produced in AD in the acidogenesis and acetogenesis step. Also, syntrophic acetogens such as special genera of clostridia can oxidize acetate to CO_2 and H_2. Then, the hydrogenotrophic methanogens produce CH_4 by utilizing H_2 and CO_2. The activity of autotrophic methanogens is restricted by the availablability of H_2 in the system [32]. Therefore, production of 1 mol autotrophic biomass is much slower than heterotrophs. Assuming H_2 is available as the electron donor (Equation (14)). The anabolic autotrophic growth was obtained as shown in Equation (26):

$$0.8\ CO_2 + 0.2\ HCO_3^- + 0.2\ NH_4^+ + 4.2\ H^+ + 4.2\ e^- \rightarrow CH_{1.8}O_{0.5}N_{0.2} + 1.7\ H_2O \quad (26)$$

Assuming the low yield, and converting it to molar unit gives:

$$Y^{Ogr}_{X,aut,meth,min} = \frac{0.05 g biomass}{g\left(CO_2/HCO_3^-\right)} \frac{1 mol biomass}{24.6 g} \frac{0.8(44 g_2) + 0.2\left(61 g HCO_3^-\right)}{1 mol\left(_2/HCO_3^-\right)} = 0.096 \frac{mol biomass}{mol carbon source}$$

The overall growth reactions (Equations (27) and (28)) were obtained for the low and high biomass yield for the formation of 1 mol autotrophic biomass using the catabolic reaction (Equation (15)) for CO_2 reduction to CH_4.

$$2.4\ CO_2 + 0.2\ HCO_3^- + 0.2\ NH_4^+ + 8.5\ H_2 \rightarrow 1.6\ CH_4 + CH_{1.8}O_{0.5}N_{0.2} + 4.9\ H_2O \quad \begin{array}{l} \Delta G^0 = -63\ \text{kJ/mol} \\ Y_{biomass,\ molar} = 0.385 \\ f_{cat} = 1.6 \end{array} \quad (27)$$

$$10.2\ CO_2 + 0.2\ HCO_3^- + 0.2\ NH_4^+ + 39.7\ H_2 \rightarrow 9.4\ CH_4 + CH_{1.8}O_{0.5}N_{0.2} + 20.5\ H_2O \quad \begin{array}{l} \Delta G^0 = -1083.8\ \text{kJ/mol} \\ Y_{biomass,\ molar} = 0.096 \\ f_{cat} = 9.41 \end{array} \quad (28)$$

3.2. Stoichiometry of Biological CO_2 to CH_4 Conversion by Approach-2

The electron equivalent of cell synthesis can be obtained from Equation (29).

$$\tfrac{4}{21}\ CO_2 + \tfrac{1}{21}\ HCO_3^- + \tfrac{1}{21}\ NH_4^+ + H^+ + e^- \rightarrow \tfrac{5}{21} CH_{1.8}O_{0.5}N_{0.2} + \tfrac{17}{42}\ H_2O \quad \Delta G^0 = +34.79\ \text{kJ/e}^-\ \text{eq} \quad (29)$$

To calculate ΔG_p, the ΔG of reduction reaction should be considered, which for H^+ to H_2 is +39.87 kJ/e$^-$ eq. The required parameters are given in Table 2. Also, Equation (15) in STD conditions was used for calculating the electron equivalent value (A).

Table 2. The calculated bioenergetic parameters required for CH_4 formation from H_2.

Electron Donor	ΔG_p(kJ/e$^-$ eq)	ΔG_{pc}(kJ/e$^-$ eq)	ε	n
H_2	35.09 − 39.87= −4.78	+34.79	0.6	−1

Substituting the values in Table 2 and using the Gibbs free energy of Equation (15) gives A = 5.62 and the bioenergetic coefficients $f_e^0 = 1 - f_s^0$ = 0.8489. For autotrophic H_2 to CH_4, the theoretical reaction (Equation (30)) based on ΔG^0 values is:

$$0.135\ CO_2 + 0.0072\ HCO_3^- + 0.0072\ NH_4^+ + 0.5\ H_2 \rightarrow 0.106\ CH_4 + 0.036\ CH_{1.8}O_{0.5}N_{0.2} + 0.27 H_2O \quad (30)$$

Therefore, for 1 mol biomass the growth reaction (Equation (31)) will be:

$$-3.75\ CO_2 - 0.2 HCO_3^- - 0.2\ NH_4^+ - 13.9\ H_2 + 2.95\ CH_4 + 1\ CH_{1.8}O_{0.5}N_{0.2} + 7.6 H_2O \quad (31)$$

The theoretical biomass yield from the stoichiometric reaction is obtained to be 0.2532 $\frac{mol\ biomass}{mol\ (CO_2/HCO_3^-)}$. Assuming the biomass yield of 0.05 $\frac{g\ biomass}{g\ (CO_2/\ HCO_3^-)}$, the corresponding f_s as $f_{s,\ real}$ can be estimated proportionally as:

$$\frac{Y_{theoretical} = 0.2535}{Y_{real} = 0.096} : \frac{f^0_{s,\ theoretical} = 0.1511}{f_{s,\ real} = ?}$$

Thus $f_{s,\ real}$ = 0.0572, which finally gives Equation (32):

$$0.13\ CO_2 + 0.0027\ HCO_3^- + 0.0027\ NH_4^+ + 0.5\ H_2 \rightarrow 0.12\ CH_4 + 0.014\ CH_{1.8}O_{0.5}N_{0.2} + 0.26\ H_2O \quad (32)$$

Equations (33) and (34) show the upscaled reactions for 1 mol biomass in STD conditions.

Approach-1:

$$10.2\ CO_2 + 0.2\ HCO_3^- + 0.2\ NH_4^+ + 39.7\ H_2 \rightarrow 9.4\ CH_4 + CH_{1.8}O_{0.5}N_{0.2} + 20.5\ H_2O \qquad \Delta G^0 = -1083.77\ \text{kJ/mol},\ Y_{biomass,\ molar} = 0.096 \quad (33)$$

Approach-2:

$$-9.5\ CO_2 - 0.2\ HCO_3^- - 0.2\ NH_4^+ - 36.7\ H_2 \rightarrow 8.6\ CH_4 + CH_{1.8}O_{0.5}N_{0.2} + 19\ H_2O \qquad \Delta G^0 = -1152.41\ \text{kJ/mol},\ Y_{biomass,molar} = 0.1 \quad (34)$$

The stoichiometric values for autotrophic reaction with approaches 1 and 2 is remarkably close. Since approach-2 is based on electron equivalent of components, it is easier to be combined with Nernst equation (Equation (19)) to obtain electric potential of the reaction. In approach-2, the number of electrons is equal to 1 in the half-reactions. According to this, the stoichiometry of bioelectrochemical anodic and cathodic reactions were assessed by implementing approach-2.

3.3. Stoichiometry of Bioelectrochemical Microbial Growth

3.3.1. Stoichiometry of the Growth of ARB

For acetate as the carbon source for ARB, the ΔG of CO_2 reduction to acetate is +27.40 kJ/e$^-$ eq. ΔG_p =+7.69 kJ/e$^-$ eq. Therefore, ΔG_s for the ARB is calculated to be 70.8 kJ/e$^-$ eq. In addition, the voltage and ΔG are limited by $A = \frac{f_e^0}{f_s^0} = \frac{-70.8}{0.6 \cdot (\Delta G_r^0)}$.

The expression shows that the A value cannot be negative. Because f_e^0 will be greater than 1 and $f_s^0 < 0$, which is not possible. Moreover, ΔG_r^0 should be negative indicating spontaneous reaction. Also, higher A is more beneficial because f_e^0 will be higher ($f_e^0 < 1$). This means the biomass yield is low, and more electrons are available for CH_4 production. Figure 2 shows cathodic voltage −0.3 V *vs*. SHE results in the highest A for anode oxidizing bacteria. All the calculated values for these thermodynamic models can be found in the Supplementary Materials Tables S1 and S2.

Figure 3 shows −0.3 V *vs*. SHE at cathode that theoretically results in +0.3 V *vs*. SHE at anode, results in the highest f_e^0 which means ARB need less substrate for maintenance. Thus, more electrons will be delivered to the anode. More negative voltage reduces f_e^0 and increases f_s^0 of ARB. Cathodic voltages more positive than −0.3 V, results in negative A value (Figure 2) which further results in $f_s^0 < 0$ that is impossible. It means that the biomass is consumed rather than it is produced. This analysis shows that even when all the potential losses in the system are ignored, the anode voltage cannot be higher than a certain value. Higher anodic voltage as the result of bigger cathodic potential, may

result in bigger f_s^0 which means less electron flow toward cathode. Nonetheless, the voltage reported for cathodes in experimental studies is more negative than −0.3 V vs. SHE, since more components are involved in oxidation. Moreover, the potential losses are higher due to complex media.

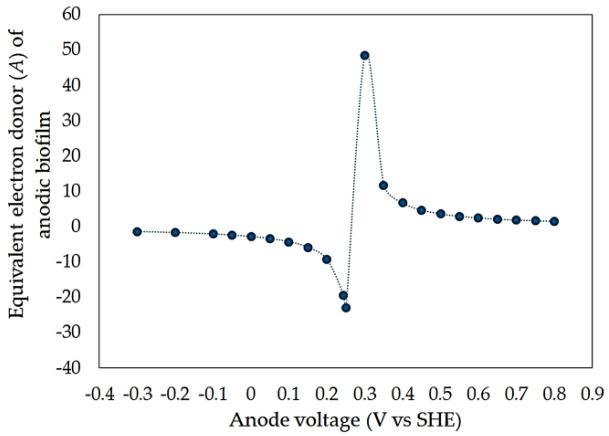

Figure 2. The equivalent electron donor value (A) for the anode voltage response −0.3 to +0.8 V *vs*. SHE.

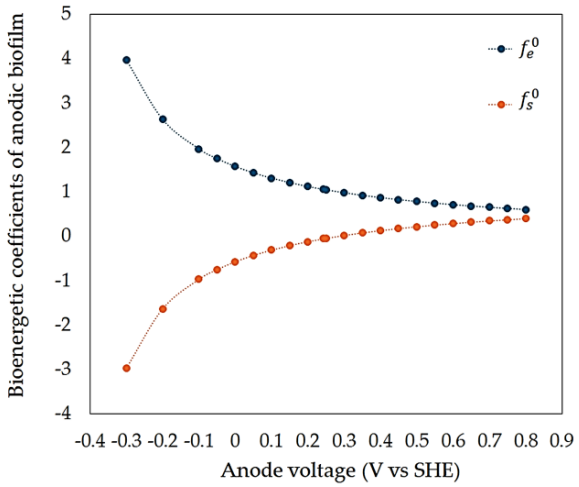

Figure 3. Bioenergetic coefficients, f_e^0 and f_s^0 for anodic biofilm metabolism at anode voltage response −0.3 to +0.8 V vs. SHE.

According to the f_e^0 and f_s^0 obtained from the applied voltage, the ARB growth reaction (Equation (35)) based on acetate consumption is:

$$-1\cdot\left(\tfrac{1}{8}CO_2+\tfrac{1}{8}HCO_3^-+H^++e^-\rightarrow\tfrac{1}{8}CH_3COO^-+\tfrac{3}{8}H_2O\right)+f_s^0\cdot\left(\tfrac{4}{21}\,CO_2+\tfrac{1}{21}\,HCO_3^-+\tfrac{1}{21}\,NH_4^++H^++e^-\rightarrow\tfrac{5}{21}CH_{1.8}O_{0.5}N_{0.2}+\tfrac{17}{42}\,H_2O\right) \quad (35)$$

Also, $+f_e^0\cdot(-e^-)$ will be delivered to anode to have a complete catabolic reaction. The stoichiometric reactions of ARB growth calculated for 3 cathodic voltages is given in Equations (36)–(38)).

$$0.125\,CH_3COO^-+0.367\,H_2O+0.001\,NH_4^+\rightarrow 0.005\,CH_{1.8}O_{0.5}N_{0.2}+0.12\,CO_2+0.124\,HCO_3^-+0.98\,H^++0.98\,e^- \quad E_{cathode}=-0.3\text{ V }vs.\text{ SHE},\ Y_{ARB,\,molar}=0.0384 \quad (36)$$

$$0.125\,CH_3COO^-+0.272\,H_2O+0.012\,NH_4^+\rightarrow 0.0605\,CH_{1.8}O_{0.5}N_{0.2}+0.076CO_2+0.113\,HCO_3^-+0.746\,H^++0.746\,e^- \quad E_{cathode}=-0.55\text{ V }vs.\text{ SHE},\ Y_{ARB,\,molar}=0.484 \quad (37)$$

$$0.125\,CH_3COO^-+0.214\,H_2O+0.019\,NH_4^+\rightarrow 0.095\,CH_{1.8}O_{0.5}N_{0.2}+0.05\,CO_2+0.12\,HCO_3^-+0.602\,H^++0.602\,e^- \quad E_{cathode}=-0.8\text{ V }vs.\text{ SHE},\ Y_{ARB,\,molar}=0.7582 \quad (38)$$

3.3.2. Stoichiometry of the Growth of Electroactive Methanogens

Figure 4 shows that the electron equivalent (A) is the highest at cathodic voltage -0.25 V *vs*. SHE for methanogenic growth. Nevertheless, the electron source is acetate oxidation at anode and the optimum A value is obtained at +0.3 V *vs*. SHE, which corresponds to -0.3 V *vs*. SHE at cathode, theoretically. Therefore, -0.25 V *vs*. SHE is too low to provide enough electrical energy to undergo acetate oxidation. Thus, the starting value for cathode will be -0.3 V *vs*. SHE. The stoichiometry of cathodic biofilm was calculated for the obtained f_e^0 and f_s^0 based on the cathodic voltage and direct CO_2 reduction to CH_4 (Figure 5). Then, the stoichiometric coefficients were calculated according to the available electrons from anode. Figure 5 shows that -0.25 V *vs*. SHE results in the highest f_e^0. This means the methanogenic anabolism needs less energy. Thus, more electrons will be available for CO_2 reduction to CH_4. However, because of anodic limitations, f_e^0 and f_s^0 obtained at -0.3 V *vs*. SHE, were the optimum bioenergetic coefficients to establish the metabolic stoichiometry of methanogens.

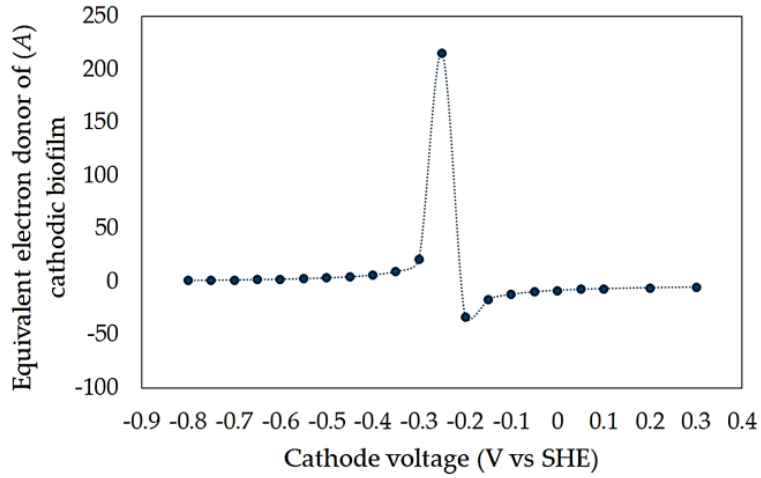

Figure 4. The equivalent electron donor value for methanogenic biofilm metabolism at different applied cathode potentials from -0.8 to +0.3 V vs. SHE.

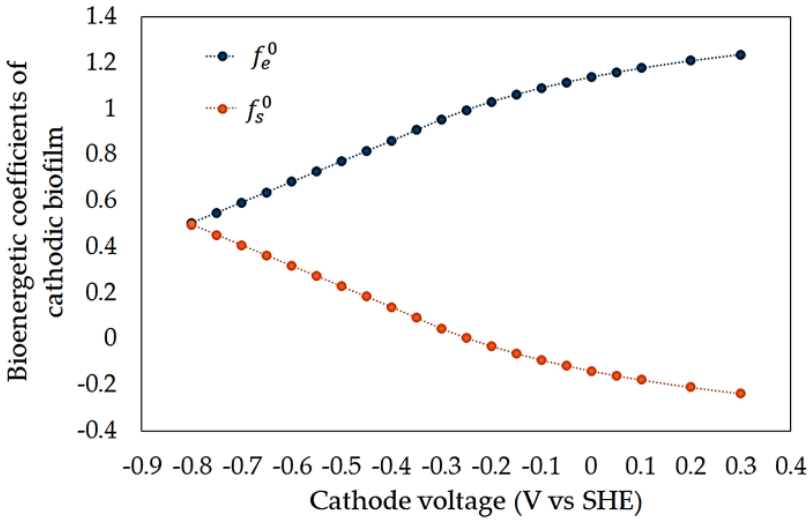

Figure 5. Bioenergetic coefficients f_e^0 and f_s^0 for methanogenic biofilm metabolism at cathode voltage -0.8 to +0.3 V vs. SHE.

The stoichiometry of metabolic reaction of electroactive methanogenic biofilm growth was established for three voltages shown in Equations (39)–(41). The electron, CO_2, and H^+ source was obtained from the oxidation of acetate via ARB. The cathodic biomass yield for different applied voltages shows that the biomass yield based on CO_2 consumption increases at higher applied voltages. The higher biomass yield is not thermodynamically beneficial because lower substrate will be available for CH_4 production.

$$0.125\ CO_2 + 0.002\ HCO_3^- + 0.98\ H^+ + 0.98\ e^- + 0.002\ NH_4^+ \rightarrow 0.011\ CH_{1.8}O_{0.5}N_{0.2} + 0.12\ CH_4 + 0.25\ H_2O \quad E_{cathode} = -0.3\ \text{V } vs.\ \text{SHE},\ Y_{ARB,\ molar} = 0.083 \tag{39}$$

$$0.107\ CO_2 + 0.01\ HCO_3^- + 0.746\ H^+ + 0.75\ e^- + 0.01 NH_4^+ \rightarrow 0.048\ CH_{1.8}O_{0.5}N_{0.2} + 0.068\ CH_4 + 0.22\ H_2O \quad E_{cathode} = -0.55\ \text{V } vs.\ \text{SHE},\ Y_{ARB,\ molar} = 0.417 \tag{40}$$

$$0.095\ CO_2 + 0.014\ HCO_3^- + 0.6\ H^+ + 0.6\ e^- + 0.014\ NH_4^+ \rightarrow 0.07\ CH_{1.8}O_{0.5}N_{0.2} + 0.038\ CH_4 + 0.2\ H_2O \quad E_{cathode} = -0.8\ \text{V } vs.\ \text{SHE},\ Y_{ARB,\ molar} = 0.65 \tag{41}$$

Figure 6 shows that the optimum anodic biomass yield can be achieved at cathodic voltage −0.3 V *vs.* SHE. At voltages lower than −0.3 V, the anodic biomass yield becomes negative which is thermodynamically impossible.

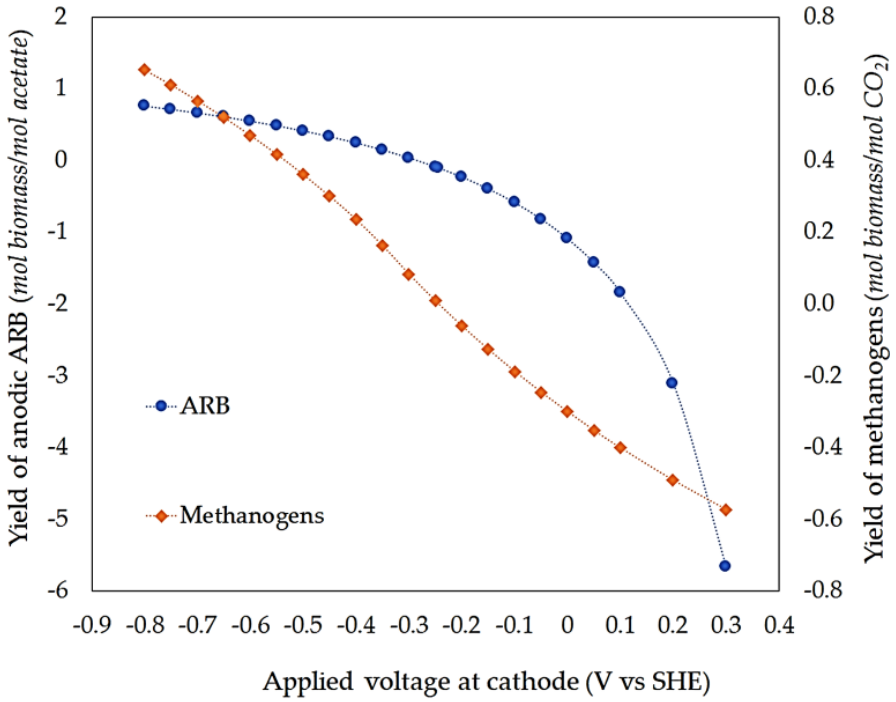

Figure 6. Biomass yield of anodic ARB on acetate consumption and methanogenic biomass yield on CO_2 consumption at cathodic voltage −0.8 to +0.3 V vs. SHE.

Figure 7 also shows that in higher voltages, more acetate is consumed for microbial cell synthesis, and less substrate and electrons will be available for CH_4 production. Since electroactive methanogens rely on electron and the substrate supply from anode, −0.3 V on cathode is optimum for the highest CH_4 production. Also due to the anodic limitations, the methanogenic biomass yield is theoretically obtained to be 0.083.

Although the model is developed for STD conditions, the results align with CH_4 yield obtained from experimental studies. In a study conducted in long term operation of heat-treated steel electrodes, lower applied voltage on cathode (−0.6 V *vs.* SHE) resulted in higher CH_4 production compared to higher voltage (−0.7 V *vs.* SHE). It is stated that higher voltage disturbed the methanogens and was not favorable for increasing CH_4 production [31]. Another research on a single chamber BES reactor with graphite felt cathode showed that −0.65 V *vs.* SHE was in favor of enhancing CH_4 evolution, while increasing the voltage to −0.8 V *vs.* SHE shifted the system toward acetic acid production [16]. Another experimental study with amended iron graphite cathode also showed that between −0.65, −0.7, −0.75, and −0.8 V *vs.* SHE, the optimum voltage for the highest CH_4 production was −0.75 V *vs.* SHE [33]. The different optimum voltages in various reactors are

due to factors such as different electrode materials, various substrates, microbial community, and conductivity in different systems which impact ionic gradients in the BES reactors [34].

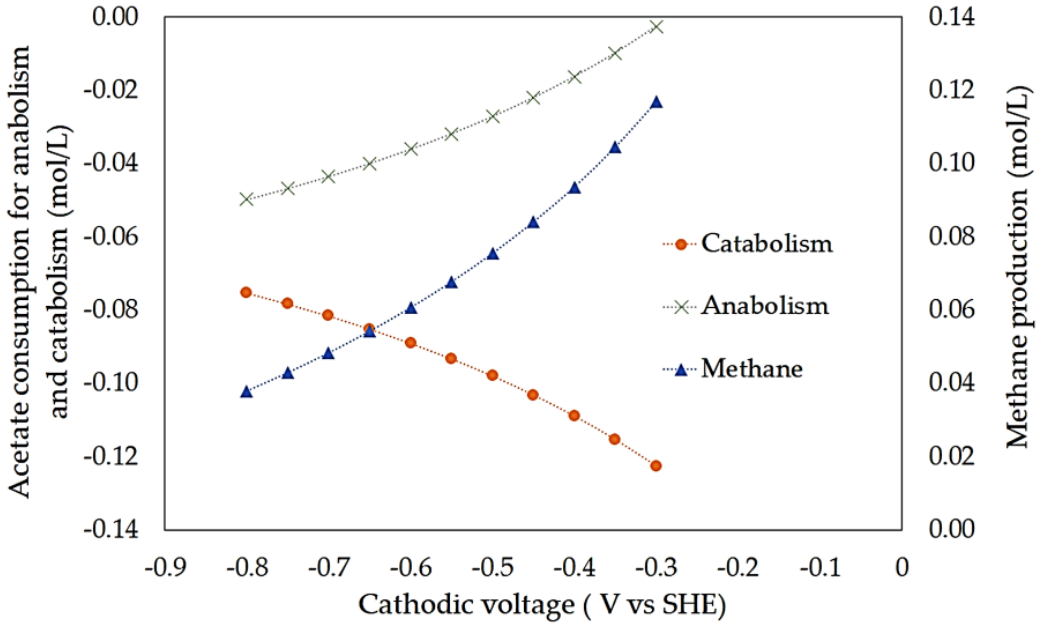

Figure 7. Acetate consumption (in negative values) for anabolism and catabolism of anodic biofilm and the maximum amount of CH_4, which could be produced from acetate oxidation.

3.3.3. Effect of Acetate Concentration at Different Temperatures

f_e^0 and f_s^0 at different acetate concentrations and temperatures is given in Table 3. According to the table, more negative voltage should be applied on cathode at lower acetate concentrations (0.0085 mol/L). The values show the optimum theoretical voltage on cathode deviates to −0.4 V *vs*. SHE from −0.3 V at STD condition (1 mol/L acetate).

Table 3. Theoretical voltages required for anodic oxidation of acetate at different concentrations and temperatures, the minimum cathode voltage, and bioenergetic coefficients of ARB.

CH_3COO^- (mol/L)	T (°C)	$E_{new,oxacetate}$ (V)	$E_{cathode}$ (V)	f_e	f_s
0.0085	25	0.368357	−0.4	0.9610	0.0390
0.0085	35	0.371187	−0.4	0.9644	0.0356
0.0085	45	0.374017	−0.4	0.9678	0.0322
0.0085	55	0.376847	−0.4	0.9712	0.0288
0.025	25	0.337177	−0.35	0.9838	0.0162
0.025	35	0.338961	−0.35	0.9860	0.0140
0.025	45	0.340745	−0.35	0.9883	0.0117
0.025	55	0.342529	−0.35	0.9905	0.0095
0.042	25	0.322182	−0.34	0.9656	0.0344
0.042	35	0.323464	−0.34	0.9671	0.0329
0.042	45	0.324745	−0.34	0.9686	0.0314
0.042	55	0.326026	−0.34	0.9702	0.0298

In addition, change in acetate concentration has more influence on applied voltage compared to temperature changes. Higher temperature increases the ARB yield, so less electrons and substrates will be released to be further consumed via methanogens at cathode. However, the effect of temperature is insignificant at higher acetate concentrations for both ARB and methanogens (Figure 8). Overall, concentration has more influence on the applied voltage. Nevertheless, f_e which is the coefficient of catabolism, increases by temperature elevation.

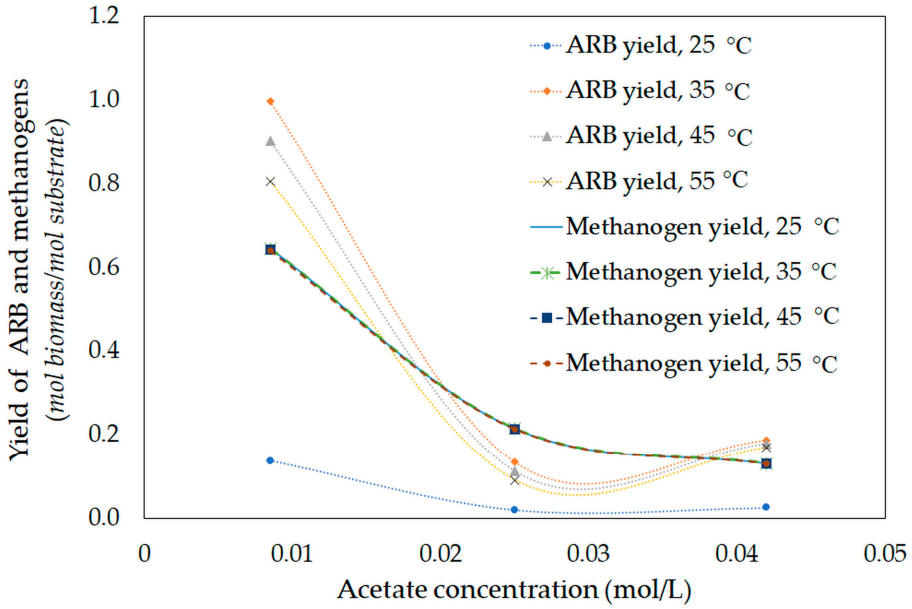

Figure 8. Yield of ARB and methanogenic biofilm at different acetate concentrations and different temperatures.

3.4. Implementing the Model in a Real BES System, Model Validation

According to the data from the reference experimental study described in Section 2.5, the SCOD and acetic acid could be the most possible feed for the anodic microbes. The stoichiometry of bioelectrochemical protein and acetate oxidation was established as given in Table 4:

Table 4. Bioenergetic coefficients calculated for experimental data at two different applied voltages.

Applied Cathodic Voltage	Microbes	f_e^0	f_s^0
−0.6 V vs. SHE	SCOD oxidizers	0.947	0.053
	Acetate oxidizers	0.9532	0.0468
	Autotrophic Methanogens	0.89	0.11
−0.7 V vs. SHE	SCOD oxidizers	0.87	0.13
	Acetate oxidizers	0.884	0.116
	Autotrophic Methanogens	0.877	0.123

At −0.6 and −0.7 V *vs*. SHE, the stoichiometry of anodic ARB for SCOD and acetate oxidizers, and the calculated yield is given by Equations (42)–(45).

$$0.015C_{16}H_{24}O_5N_4 + 0.0025HCO_3^- + 0.3877H_2O \rightarrow 0.0126CH_{1.8}O_{0.5}N_{0.2} + 0.058NH_4^+ + 0.2324CO_2 + 0.886H^+ + 0.947e^- \quad E_{cathode} = -0.6\text{ V } vs.\text{ SHE},\ Y_{SCOD\ oxidizers,\ molar} = 0.84 \tag{42}$$

$$0.125CH_3COO^- + 0.356H_2O + 0.0022NH_4^+ \rightarrow 0.011CH_{1.8}O_{0.5}N_{0.2} + 0.1161CO_2 + 0.1228HCO_3^- + 0.9532H^+ + 0.953e^- \quad E_{cathode} = -0.6\text{ V } vs.\text{ SHE},\ Y_{Acetate\ oxidizers,\ molar} = 0.088 \tag{43}$$

$$0.015C_{16}H_{24}O_5N_4 + 0.0062HCO_3^- + 0.356H_2O \rightarrow 0.031CH_{1.8}O_{0.5}N_{0.2} + 0.054NH_4^+ + 0.2176CO_2 + 0.81H^+ + 0.87e^- \quad E_{cathode} = -0.7\text{ V } vs.\text{ SHE},\ Y_{SCOD\ oxidizers,\ molar} = 2.06 \tag{44}$$

$$0.125CH_3COO^- + 0.953H_2O + 0.0055NH_4^+ \rightarrow 0.0276CH_{1.8}O_{0.5}N_{0.2} + 0.103CO_2 + 0.119HCO_3^- + 0.884H^+ + 0.884e^- \quad E_{cathode} = -0.7\text{ V } vs.\text{ SHE},\ Y_{Acetate\ oxidizers,\ molar} = 0.221 \tag{45}$$

The methanogenic growth stoichiometry with molar biomass and CH_4 production yield can be seen in Equations (46) and (47).

$$0.132CO_2 + 0.0052\ HCO_3^- + 0.0052NH_4^+ + H^+ + e^- \rightarrow 0.0262CH_{1.8}O_{0.5}N_{0.2} + 0.111CH_4 + 0.267H_2O \quad \begin{matrix} E_{cathode} = -0.6\ \text{V}\ vs.\ \text{SHE} \\ Y_{Methanogens,\ molar} = 0.19 \\ Y_{CH_4,\ molar} = 0.81 \end{matrix} \quad (46)$$

$$0.133CO_2 + 0.0085\ HCO_3^- + 0.0085NH_4^+ + H^+ + e^- \rightarrow 0.029CH_{1.8}O_{0.5}N_{0.2} + 0.109CH_4 + 0.269H_2O \quad \begin{matrix} E_{cathode} = -0.7\ \text{V}\ vs.\ \text{SHE} \\ Y_{Methanogens,\ molar} = 0.205 \\ Y_{CH_4,\ molar} = 0.77 \end{matrix} \quad (47)$$

The model in the complex system shows that the molar biomass yield increases when higher electric potential is applied to cathode, while molar CH_4 yield decreases at higher voltage. This model thermodynamically proves that -0.6 V *vs*. SHE is the optimum voltage for CH_4 production, which aligns with the results of this experimental study. The model is valid for implementation in real systems with multiple substrates, considering ohmic losses due to many factors such as non-STD conditions, electrode intrinsic potential and mixed microbial environment.

4. Conclusions

The overall growth response of anodic and cathodic microbial biofilm gives essential system operating data. It enables us to determine the acid/base dose requirements for nutritional requirements per unit of electron donor and pH regulation. Also, it makes it simple to calculate the thermodynamic characteristics of the system. For the growth of 1 mol biomass, the stoichiometric coefficients obtained by both empirical and theoretical approaches were almost similar. While the empirical approach is more straightforward to calculate the stoichiometries of growth, relating ΔG_s to ΔE by Nernst equation is easier by the theoretical approach. Therefore, a theoretical approach which is based on the electron equivalent of the reaction, can be used to establish the stoichiometry of electroactive biofilms. The model showed that more negative voltage (higher energy input) on cathode should be applied when the acetate concentration is lower than the STD amount (1 mol/L). The thermodynamic model showed that the applied voltage in a bioelectrochemical reactor for CH_4 recovery depends highly on the concentration of organic substrate, even if ohmic losses are ignored. Higher temperature helps for better performance at lower organic concentrations. To have energy-efficient process, temperature and voltage can be regulated according to the availability of organic substrate for bioanode. Implementing the thermodynamic model using accurate data, aligned with experimental results, proves that the model can be used as an accurate tool for microbial biomass and CH_4 yield prediction, enabling more effective system design and operation. By enhancing predictions of biofilm growth dynamics, this approach supports the development of more energy-efficient BES configurations for sustainable CH_4 recovery.

Supplementary Materials: The following supporting information can be downloaded at: https://www.mdpi.com/article/10.3390/fermentation11010040/s1, Table S1: The calculated parameters to establish the stoichiometry of ARB growth at anode when the bioelectrochemical reactor is controlled by different cathodic potentials.; Table S2: The calculated parameters to establish the stoichiometry of electroactive methanogens at cathode at different cathodic potentials. Electrons and H^+ is generated at anode. title; Table S3: Gibbs free energy of formation of different components.

Author Contributions: V.A.: Conceptualization, methodology, software, validation, investigation, writing—original draft preparation; N.A.: data validation, review and editing, administration. All authors have read and agreed to the published version of the manuscript.

Funding: This research was funded by the University of Southeastern Norway via KD program, grant number 6042927.

Institutional Review Board Statement: Not applicable.

Informed Consent Statement: Not applicable.

Data Availability Statement: The original contributions presented in the study are included in the article and Supplementary Materials; further inquiries can be directed to the authors.

Conflicts of Interest: The authors declare no conflicts of interest.

References

1. Li, Z.; Fu, Q.; Su, H.; Yang, W.; Chen, H.; Zhang, B.; Hua, L.; Xu, Q. Model development of bioelectrochemical systems: A critical review from the perspective of physiochemical principles and mathematical methods. *Water Res.* **2022**, *226*, 119311. [CrossRef]
2. Jadhav, G.S.; Jagtap, Y.D.; Bhowmick, G.D.; Ghangrekar, M.M. Modelling of Bioelectrochemical Systems: Biophysicochemical Processes and Mathematical Methods. *Microb. Electrochem. Technol. Fundam. Appl.* **2023**, *2*, 529–554.
3. Mullai, P.; Vishali, S.; Sambavi, S.; Dharmalingam, K.; Yogeswari, M.; Raja, V.V.; Bharathiraja, B.; Bayar, B.; Abubackar, H.N.; Al Noman, A.; et al. Energy generation from bioelectrochemical techniques: Concepts, reactor configurations and modeling approaches. *Chemosphere* **2023**, *342*, 139950. [CrossRef] [PubMed]
4. Luo, S.; Wang, Z.-W.; He, Z. Mathematical modeling of the dynamic behavior of an integrated photo-bioelectrochemical system for simultaneous wastewater treatment and bioenergy recovery. *Energy* **2017**, *124*, 227–237. [CrossRef]
5. Mais, L.; Rodriguez, J.; Melis, N.; Vacca, A.; Mascia, M. Computational modelling as a design tool for bioelectrochemical systems. *Curr. Opin. Electrochem.* **2024**, *44*, 101460. [CrossRef]
6. Ahmadi, V.; Dinamarca, C. Simulation of the Effect of Local Electric Potential and Substrate Concentration on CO_2 Reduction via Microbial Electrosynthesis. In Proceedings of the 63rd International Conference of Scandinavian Simulation Society, SIMS 2022, Trondheim, Norway, 20–21 September 2022.
7. Capodaglio, A.G.; Cecconet, D.; Molognoni, D. An integrated mathematical model of microbial fuel cell processes: Bioelectrochemical and microbiologic aspects. *Processes* **2017**, *5*, 73. [CrossRef]
8. Deb, D.; Patel, R.; Balas, V.E. A review of control-oriented bioelectrochemical mathematical models of microbial fuel cells. *Processes* **2020**, *8*, 583. [CrossRef]
9. Nwokolo, N.; Mukumba, P.; Obileke, K.; Enebe, M. Waste to energy: A focus on the impact of substrate type in biogas production. *Processes* **2020**, *8*, 1224. [CrossRef]
10. Uddin, M.M.; Wright, M.M. Anaerobic digestion fundamentals, challenges, and technological advances. *Phys. Sci. Rev.* **2023**, *8*, 2819–2837. [CrossRef]
11. Lin, R.; Cheng, J.; Ding, L.; Murphy, J.D. Improved efficiency of anaerobic digestion through direct interspecies electron transfer at mesophilic and thermophilic temperature ranges. *Chem. Eng. J.* **2018**, *350*, 681–691. [CrossRef]
12. Aryal, N.; Ghimire, N.; Bajracharya, S. Coupling of microbial electrosynthesis with anaerobic digestion for waste valorization. *Adv. Bioenergy* **2020**, *5*, 101–127.
13. Aryal, N.; Zhang, Y.; Bajracharya, S.; Pant, D.; Chen, X. Microbial electrochemical approaches of carbon dioxide utilization for biogas upgrading. *Chemosphere* **2022**, *291*, 132843. [CrossRef] [PubMed]
14. Aryal, N.; Ammam, F.; Patil, S.A.; Pant, D. An overview of cathode materials for microbial electrosynthesis of chemicals from carbon dioxide. *Green. Chem.* **2017**, *19*, 5748–5760. [CrossRef]
15. Metcalf & Eddy Inc. *Wastewater Engineering: Treatment and Resource Recovery*; McGraw Hill Education: New York, NY, USA, 2014.
16. Nelabhotla, A.B.T.; Dinamarca, C. Bioelectrochemical CO_2 reduction to methane: MES integration in biogas production processes. *Appl. Sci.* **2019**, *9*, 1056. [CrossRef]
17. Rittmann, B.E.; McCarty, P.L. *Microbial Electrochemical Cells*, 2nd ed.; McGraw-Hill Education: New York, NY, USA, 2020; Available online: https://www.accessengineeringlibrary.com/content/book/9781260441604/back-matter/appendix4 (accessed on 9 January 2025).
18. Ware, A.; Power, N. Modelling methane production kinetics of complex poultry slaughterhouse wastes using sigmoidal growth functions. *Renew. Energy* **2017**, *104*, 50–59. [CrossRef]
19. Heijnen, J.J.; Kleerebezem, R. Bioenergetics of microbial growth. *Encycl. Bioprocess Technol. Ferment. Biocatal. Biosep.* **1999**, *1*, 267–291.
20. Rittmann, B.E.; McCarty, P.L. *Environmental Biotechnology: Principles and Applications*; McGraw-Hill: New York, NY, USA, 2001.
21. Korth, B.; Rosa, L.F.M.; Harnisch, F.; Picioreanu, C. A framework for modeling electroactive microbial biofilms performing direct electron transfer. *Bioelectrochemistry* **2015**, *106*, 194–206. [CrossRef] [PubMed]
22. Quéméner, E.D.-L.; Moscoviz, R.; Bernet, N.; Marcus, A. Modeling of interspecies electron transfer in anaerobic microbial communities. *Curr. Opin. Biotechnol.* **2021**, *67*, 49–57. [CrossRef] [PubMed]
23. Marcus, A.K.; Torres, C.I.; Rittmann, B.E. Conduction-based modeling of the biofilm anode of a microbial fuel cell. *Biotechnol. Bioeng.* **2007**, *98*, 1171–1182. [CrossRef]
24. Torres, C.I.; Marcus, A.K.; Parameswaran, P.; Rittmann, B.E. Kinetic Experiments for Evaluating the Nernst−Monod Model for Anode-Respiring Bacteria (ARB) in a Biofilm Anode. *Environ. Sci. Technol.* **2008**, *42*, 6593–6597. [CrossRef]
25. Thauer, R.K.; Kaster, A.-K.; Seedorf, H.; Buckel, W.; Hedderich, R. Methanogenic archaea: Ecologically relevant differences in energy conservation. *Nat. Rev. Microbiol.* **2008**, *6*, 579–591. [CrossRef]

26. Tremblay, P.-L.; Faraghiparapari, N.; Zhang, T. Accelerated H_2 evolution during microbial electrosynthesis with Sporomusa ovata. *Catalysts* **2019**, *9*, 166. [CrossRef]
27. Smith, J.M. *Introduction to Chemical Engineering Thermodynamics*; ACS Publications: Washington, DC, USA, 1950.
28. Rittmann, B.E.; McCarty, P.L. *Environmental Biotechnology: Principles and Applications*, 2nd ed.; McGraw-Hill Education: New York, NY, USA, 2020; Available online: https://www.accessengineeringlibrary.com/content/book/9781260441604 (accessed on 1 June 2021).
29. Flowers, P.; Theopold, K.H.; Langley, R.; Neth, E.J.; Robinson, W.R. *Chemistry: Atoms First 2e*; OpenStax, Rice University: Houston, TX, USA, 2019.
30. Zeitz, J.O.; Bucher, S.; Zhou, X.; Meile, L.; Kreuzer, M.; Soliva, C.R. Inhhibitory effects of saturated fatty acids on methane production by methanogenic Archaea. *J. Anim. Feed. Sci.* **2013**, *22*, 44–49. [CrossRef]
31. Ahmadi, V.; Dinamarca, C.; Aryal, N. Durability and mass loss effect of heat-treated stainless-steel cathode for methane production from organic and inorganic carbon in a bioelectrochemical system. *J. Hazard. Mater. Adv.* **2025**, *17*, 100573. [CrossRef]
32. Mand, T.D.; Metcalf, W.W. Energy Conservation and Hydrogenase Function in Methanogenic Archaea, in Particular the Genus Methanosarcina. *Microbiol. Mol. Biol. Rev.* **2019**, *83*, e00020-19. [CrossRef] [PubMed]
33. Dykstra, C.M.; Pavlostathis, S.G. Zero-valent iron enhances biocathodic carbon dioxide reduction to methane. *Environ. Sci. Technol.* **2017**, *51*, 12956–12964. [CrossRef]
34. Aryal, N.; Feng, L.; Wang, S.; Chen, X. Surface-modified activated carbon for anaerobic digestion to optimize the microbe-material interaction. *Sci. Total Environ.* **2023**, *886*, 163985. [CrossRef]